

## Kinetic Models of Exopolysaccharide Production by *Haemophilus Influenzae* Type B

Cintra FO and Takagi M\*

Chemical Processes Development Laboratory, Development and Innovation Center, Brazil

### ARTICLE INFO

Received Date: January 03, 2022

Accepted Date: January 28, 2022

Published Date: January 30, 2022

### KEYWORDS

Haemophilus influenza  
Immunization  
Streptococcus zooepidemicus  
Cetyltrimethylammonium

**Copyright:** © 2022 Takagi M et al., SL Vaccines And Vaccination Journal. This is an open access article distributed under the Creative Commons Attribution License, which permits unrestricted use, distribution, and reproduction in any medium, provided the original work is properly cited.

**Citation for this article:** Cintra FO and Takagi M. Kinetic Models of Exopolysaccharide Production by *Haemophilus Influenzae* Type B. SL Vaccines And Vaccination Journal. 2022; 3(1):114

### Corresponding author:

Takagi M,  
Chemical Processes Development  
Laboratory, Development and  
Innovation Center, Brazil,  
Email: mickie.takagi@butantan.gov.br

### ABSTRACT

*Haemophilus influenzae* type b (Hib) is a pathogenic bacterium responsible for meningitis in infants and elderly. The polysaccharide present in the extracellular layer of the bacterium is an efficient antigen for vaccination when conjugated to a carrier protein. Immunization against Hib is encouraged to be extended in the developing countries, which sets a high demand on the production of the polysaccharide. The fermentation of Hib is unable to achieve high cell densities, probably due to accumulation of toxic compounds in the broth, decreasing greatly the polysaccharide production yields. In this work, a set of mathematical models were fitted to the experimental data of Hib growth in order to evaluate the kinetics of production of biomass, polysaccharide and acids as byproducts. The best model was chosen by model comparison and allowed us to conclude that polysaccharide formation is exclusively non-associated to growth but inhibited by acid, while acid formation follows a mixed associated and non-associated pattern. These results suggest the model 5.D as mathematical model to predict the fermentation kinetics process of *H. influenzae*.

### INTRODUCTION

Gram negative bacterium *Haemophilus influenzae* is one of the major etiological agents of infectious diseases in infants and elderly, the manifestations of which include pneumonia, septicemia and meningitis [1,2]. *H. influenzae* type b (Hib) is the most virulent and epidemiologically prevalent and the vaccine is based on capsular polysaccharide, a linear chain of poly-ribosyl-ribitol-phosphate - PRP, chemically conjugated to a carrier protein [3,4].

Hib is a fastidious organism that demands the use of complex medium and growth factors. Besides, the few fermentation processes described in the literature are usually unable to achieve high PRP production yields in a manner that is efficiently viable. Processes described are usually simple batches with no feeding carried out for short periods, and the few additional mass of PRP obtained by feeding, associated with increase of fermentation time and equipment which does not compensate the extra costs of production [5].

Hib's deficient genome includes several deletions on its metabolic pathways, which not only results in the need of complex components, but also leads to the accumulation of toxic byproducts, such as organic acids, which it is not reused in the metabolism. The low yields of PRP production and the inability to achieve high cell densities signs to the phenomenon of metabolic inhibition by these toxic compounds. Liu *et al.* [6]

demonstrated that growth other fastidious polysaccharide producing bacterium as *Streptococcus zooepidemicus* is affected by the accumulation of lactate, with a negative effect on the rates of biomass and polysaccharide synthesis.

The inhibition effects on microbial growth have been studied by the mathematical modeling of experimental data such as the one Aiba and Shoda [7]. In this model, an increase in the concentration of product is followed by a decrease in the specific rate of growth. The negative effect caused by acid may also act on the synthesis of other products or even itself. The different magnitude of the inhibition constants on cell growth and metabolite synthesis enables a better understanding of the growth kinetics and a more efficient search for the optimum process conditions. Mathematical kinetics models are widely used for the simulation and understanding of processes, however there are no studies with the polysaccharide of *Haemophilus influenzae* b.

In this work, different mathematical models considering the inhibition effects was evaluated as a tool to understand the low yields on cell growth and polysaccharide formation, and improve them.

## MATERIALS AND METHODS

Strain *Haemophilus influenzae* type b GB 3291 was obtained from the Brazilian National Center of Meningitis, Adolfo Lutz Institute, Department of Bacteriology, São Paulo, Brazil. A volume of 200mL MMP medium containing was distributed in Erlenmeyer's flasks, inoculated with a suspension of Hib ( $1.5 \times 10^{-9}$  UFC/mL) under overnight agitation of 200RPM at 37 °C resulting OD<sub>540 nm</sub> of 9 absorbance units AU) and inoculated further in bioreactor to achieve initial OD<sub>540 nm</sub> of 0.1 AU.

Cultivations were conducted in a Bio Flo 2000 bioreactor (New Brunswick Scientific) with a working volume of 6 liters, at 32°C; pH controlled at 7.0 with sodium hydroxide 5M; aeration was maintained at 0.5VVM and pO<sub>2</sub> controlled by agitation at 30% of air saturation. Modified MP medium (MMP) as described by Takagi *et al.* [8] was used in the batch phase, and for feeding MMP medium was incremented with glucose – Merck (37.5%) and yeast extract - BD (18.75%). Feeding was added as a pulse of about 80 mL upon complete exhaustion of the glucose (evaluated by a pO<sub>2</sub> spike). Samples taken from the reactor were centrifuged at 16,000g for 10 minutes at 4°C. The supernatant was frozen at -20°C for further analysis.

The cell pellets were washed with NaCl 150mM and dried at 60°C for 48h for dry cell measurements. The residual glucose was determined by the glucose oxidase/peroxidase method [9]. The acid was estimated by tracking the mass of NaOH added to the broth: the mass added at each moment was converted to an equivalent unit of H<sup>+</sup> by considering the density and concentration of the alkali solution and the total medium volume. PRP was determined by the methods described in Cintra and Takagi [10], where the supernatant of culture broth was Cetyltrimethylammonium Bromide (CTAB) precipitation - three volumes of CTAB 0.66% were added to 1 volume of the sample; the mixture was left to stand for 10 min at room temperature, and centrifuged at 15,000g for 10min; pellets were washed with pure water and resuspended in 1M NaCl [11] and the ribose content was determined by the modified Bial's method [12]; and the polysaccharide was determined multiplying the ribose content by 2.5.

Mathematical models: to describe cell growth, the model described by Aiba and Shoda [7] was used, which expands the Monod equation to determine the rate of growth considering inhibition of organic acids:

$$\frac{dX}{dt} = \left( \frac{\mu_{max} S}{K_s + S} \right) \left( \frac{1}{1 + A_c / K_{Ac \rightarrow X}} \right) X \quad (1)$$

To describe product formation (for both polysaccharide and acids), Luedeking and Piret [13] introduce an equation that states that the rate of a generic product formation is proportional to the rate of cell growth and cell concentration. Their equation was extended by including an acid inhibition term, as specified in Equation 2:

$$\frac{dQ}{dt} = \left( \frac{1}{1 + A_c / K_{Ac \rightarrow Q}} \right) \left( \alpha_Q \frac{dX}{dt} + \beta_Q X \right) \quad (2)$$

Substrate consumption was modeled by Equation 3, which was modified from the maintenance equation of Pirt [14]:

$$\frac{dS}{dt} = -\alpha_S \frac{dX}{dt} - \beta_S X \quad (3)$$

where  $\alpha_S$  represents a summation of all substrate consumed in the synthesis of biomass and other growth associated compounds, and  $\beta_S$  represents the sum of substrate consumed in cell maintenance and formation of non-associated metabolites.

To compare each model and to decide which is the most appropriate, the evidence ratio between each alternative was determined using Akaike's Information Criterion (AIC) as described by Motulsky and Christopoulos [15].

**RESULTS AND DISCUSSION**

A simple batch culture of Hib was carried out with initial glucose concentrations of 5g.L<sup>-1</sup>. Cell growth proceeded until approximately 8 hours, when glucose was totally consumed. At this point a feed pulse with concentrated glucose and yeast extract was added to the broth in order to restore the initial substrate concentration. This second phase proceeded for about 3.5 hours, when a new feed addition was applied. Fermentation was finished when this second glucose feed was depleted. Biomass achieved a final concentration of 6.62 g.L<sup>-1</sup>, with production of 727.36 mg.L<sup>-1</sup> of PRP and 104.62 mM of acid.

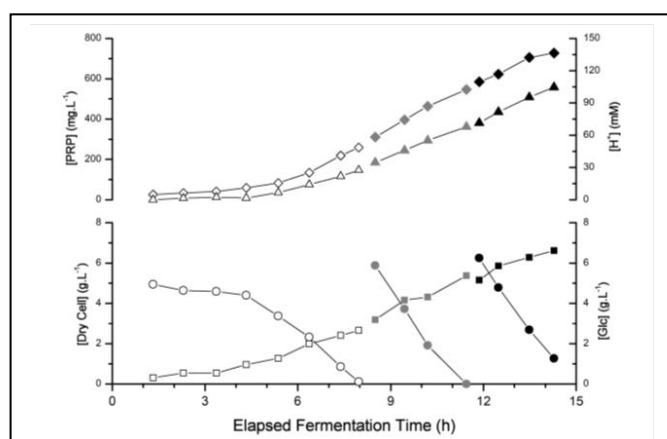


Figure 1: Experimental data of Hib fermentation with two pulsed feed addition. □: dry cell (g.L<sup>-1</sup>); ○: residual glucose (g.L<sup>-1</sup>); △: acid (mM); ◇: PRP (mg.L<sup>-1</sup>); white: first batch, gray: after the first pulse, black: after the second pulse. Only averaged values are shown.

Figure 1 depicts the overall fermentation kinetics. During the cultivation, the volume in the bioreactor changes by the addition of the fresh medium causing dilution of the components, thus every time a feed medium was added, a new batch phase was considered to start. The regression algorithm was set to determine freely the initial values of the fermentation variables after each pulse, although the kinetic parameters were considered to be the same for all the sets.

A series of mathematical models of microbial growth were considered in an effort to describe the batch culture of *H.*

*influenzae b* and its kinetics of cell growth, PRP and acid production and substrate uptake. The models applied to the experimental data were constructed as follows: Equations 1 and 3 were used to fit the model to the biomass and substrate data, respectively; as to acid data, six variations of Equation 2 were tested in order to determine the most appropriate formation kinetics. To each variation a model number was addressed, which will be used further to discuss the results. Table 1 states each of the equations for the modeling of acid formation their description.

Table 1: Equations for the modeling of acid formation.		
Model	Equation	Type
1	$\frac{dAc}{dt} = \alpha_{Ac} \frac{dX}{dt}$	Growth-associated ( $\beta_{Ac} = 0$ )
2	$\frac{dAc}{dt} = \beta_{Ac} X$	Non-growth-associated ( $\alpha_{Ac} = 0$ )
3	$\frac{dAc}{dt} = \left( \frac{1}{1 + Ac/K_{Ac \rightarrow Ac}} \right) \alpha_{Ac} \frac{dX}{dt}$	Growth-associated with inhibition by acid
4	$\frac{dAc}{dt} = \left( \frac{1}{1 + Ac/K_{Ac \rightarrow Ac}} \right) \beta_{Ac} X$	Non-growth-associated with acid inhibition
5	$\frac{dAc}{dt} = \alpha_{Ac} \frac{dX}{dt} + \beta_{Ac} X$	Mixed ( $\alpha_{Ac}, \beta_{Ac} \neq 0$ )
6	$\frac{dAc}{dt} = \left( \frac{1}{1 + Ac/K_{Ac \rightarrow Ac}} \right) (\alpha_{Ac} \frac{dX}{dt} + \beta_{Ac} X)$	Mixed with acid inhibition

The resolution of the acid equations (Table 1), biomass (Equation 1), and substrate (Equation 3) are interdependent, so all the respective parameters were obtained simultaneously, for each model. Models for PRP kinetics were assessed later, whereas neither of these equations depends on polysaccharide concentration. Table 2 shows the values obtained by regression to the experimental data for each model.

Table 2: Parameters obtained from the models used for acid formation.						
Model	1	2	3	4	5	6
$\mu_{max}$	0.488	0.406	0.488	0.412	0.418	0.412
KS	0.116	0.411	0.116	0.303	0.348	0.303
$K_{Ac \rightarrow X}$	24.759	35.671	24.759	33.713	33.325	33.713
$\alpha_{Ac}$	12.372	--	12.372	--	2.052	0.000
$\beta_{Ac}$	--	2.623	--	3.101	2.247	3.101
$K_{Ac \rightarrow Ac}$	--	--	$\infty$	335.200	--	335.200
$\alpha_S$	1.190	1.210	1.190	1.203	1.176	1.203
$\beta_S$	0.233	0.226	0.233	0.228	0.231	0.228

The acid inhibition constant ( $K_{Ac \rightarrow Ac}$ ) obtained in model 3 diverged to infinity, so this model be considered the same as model 1. Similarly, the cell growth associated constant for acid formation ( $\alpha_{Ac}$ ) described by the model 6 converged to zero, therefore this model became equivalent to model 4. Thereat, models 3 and 6 were removed from further analysis.

To assess which model describes the data more accurately, the evidence ratio between each model was calculated separately for the biomass, substrate and acid data sets, as shown on the Table 3. The numbers on the table show the likelihood that the models on the vertical position are more adequate than the ones on the horizontal position.

Table 3: Evidence ratios between models evaluated for each variable.							
a) Biomass				b) Substrate			
Model	2	4	5	Model	2	4	5
1	7.91E-01	2.06E+00	2.13E+00	1	1.79E-01	6.77E-01	7.46E-01
2		2.60E+00	2.70E+00	2		3.77E+00	4.16E+00
4			1.04E+00	4			1.10E+00

c) Acid			
Model	2	4	5
1	1.60E-07	5.05E-09	1.82E-08
2		3.16E-02	1.14E-01
4			3.60E+00

The evidence ratio is assumed to be meaningful when its order of magnitude is greater than 2, either positive or negative [15]. Tables 3.a and 3.b show that none of the evidence ratios calculated were great enough to indicate which model is more appropriate when concerning biomass and substrate. This means that the errors of all the models are comparable, i.e., all the four models are equally capable of predicting the biomass and substrate curves. Although, Table 3.c shows that model 1 describes the acid curve much less accurately than models 2, 4 and 5, so it may be discarded. The evidence ratios between models 2 and 4 and between model 2 and 5 are not small enough to assure the elimination of model 2, so it is not clear whether this model is in fact inadequate. The number of data points for the acid curve is very limited (because no replicate measurements could be made) and close to the number of parameters; therefore, the moderate values of the evidence ratio may be underestimated, and in this was model 2 was also discarded. Models 4 and 5 cannot be distinguished by the evidence ratio, and seemingly describe the data with the same

quality. Thereafter, both models were considered in the further analysis, the determination of the model for polysaccharide synthesis.

PRP is the second product of Hib metabolism that is considered in the modeling, and the equations that can be used to predict its formation also derive from Equation 3. As with acid formation, all the possible combinations of the parameters to have a more accurate result were evaluated. Table 4 resumes the possibilities tested. To avoid confusion, the models for polysaccharide formation are represented by letters.

Table 4: Models evaluated for polysaccharide formation.		
Model	Equation	Type
A	$\frac{dP_s}{dt} = \alpha_{P_s} \frac{dX}{dt}$	Growth-associated ( $\beta_{P_s} = 0$ )
B	$\frac{dP_s}{dt} = \beta_{P_s} X$	Non-growth-associated ( $\alpha_{P_s} = 0$ )
C	$\frac{dP_s}{dt} = \left( \frac{1}{1 + Ac/K_{Ac \rightarrow P_s}} \right) \alpha_{P_s} \frac{dX}{dt}$	Growth-associated with inhibition by acid
D	$\frac{dP_s}{dt} = \left( \frac{1}{1 + Ac/K_{Ac \rightarrow P_s}} \right) \beta_{P_s} X$	Non-growth-associated with acid inhibition
E	$\frac{dP_s}{dt} = \alpha_{P_s} \frac{dX}{dt} + \beta_{P_s} X$	Mixed ( $\alpha_{P_s}, \beta_{P_s} \neq 0$ )
F	$\frac{dP_s}{dt} = \left( \frac{1}{1 + Ac/K_{Ac \rightarrow P_s}} \right) \left( \alpha_{P_s} \frac{dX}{dt} + \beta_{P_s} X \right)$	Mixed with acid inhibition

To evaluate each possibility, models 4 and 5 were used separately to simulate the biomass and acid curves. Equations on Table 4 were regressed to the PRP experimental data by using the model values for biomass and acid. Twelve complete models were then constructed by the combination of models 4 and 5 from the acid models and the PRP models. Table 5 shows the values of the polysaccharide constants for each of these models. Again, some of the models became equivalent to others. In models 4.C and 5.C, the acid inhibition constant diverged to infinity, so these models became the same as models 4.A and 5.A, respectively. In models 4.F and 5.F, the growth-associated constant converged to zero, making the models equivalent to models 4.D and 5.D. These models were eliminated in the following analysis.

To evaluate which model describes the PRP kinetics more precisely, the evidence ratio between each model was calculated in the same manner as before (with respect to the

PRP data set). For sake of simplicity, models derived from model 4 were compared separately from those derived from model 5.

**Table 5: Values of the coefficients of PRP models.**

Model	$\alpha_{PS}$	$\beta_{PS}$	$K_{Ac \rightarrow PS}$
4.A	95.34	--	--
4.B	--	15.91	--
4.C	95.34	--	$\infty$
4.D	--	31.41	56.53
4.E	78.18	3.98	--
4.F	0.00	31.41	56.53
5.A	94.72	--	--
5.B	--	15.90	--
5.C	94.72	--	$\infty$
5.D	--	31.15	57.10
5.E	76.86	4.15	--
5.F	0.00	31.15	57.10

Results from Table 6 show that both models A (4.A and 5.A) are more adequate than models B, but neither are adequate when compared to models D and E, so they were excluded; models E are, by themselves, much less adequate than models D. Thus, there is great evidence that PRP formation is non-associated to growth and is inhibited by acid accumulation.

**Table 6: Evidence ratios for the PRP models.**

Model	a)			b)			
	4.B	4.D	4.E	Model	5.B	5.D	5.E
4.A	7.8E+09	1.0E-04	2.1E-02	5.A	3.4E+09	4.9E-05	1.4E-02
4.B		1.3E-14	2.7E-12	5.B		1.4E-14	4.0E-12
4.D			2.0E+02	5.D			2.8E+02

Between these two possible complete models (4.D and 5.D), the evidence ratio was calculated as only 0.81, what does not allow any conclusion. Thus, the consistency of each model was estimated by the deviations of the model parameters. This procedure was done by bootstrapping the errors in the experimental data and regressing the models to the simulated data set. Table 7 resumes, for each model, all the constants obtained by regression and the 95% confidence interval obtained by the bootstrap iterations.

Except for the acid formation parameters, it can be observed that the values obtained by regression did not differ sensibly between the two models, and that the deviation values estimated were virtually the same. To evaluate the differences between the two models, Figure 2 shows the whole histograms of the acid parameters distribution for both models.

**Table 7: Resume of model parameters and respective 95% confidence intervals.**

Parameter	Model 4.D		Model 5.D	
	Regression value	CI 95%	Regression value	CI 95%
$\mu_{max}$	0.412	(0.372 ; 0.738)	0.418	(0.349 ; 0.710)
$K_S$	0.303	(0.024 ; 2.778)	0.348	(0.016 ; 2.649)
$K_{Ac \rightarrow X}$	33.713	(22.399 ; 49.350)	33.325	(24.712 ; 52.385)
$\beta_P$	31.415	(27.897 ; 36.021)	31.149	(28.114 ; 36.318)
$K_{Ac \rightarrow P}$	56.527	(41.899 ; 84.589)	57.102	(41.692 ; 84.847)
$\alpha_{Ac}$			2.052	(0.363 ; 8.041)
$\beta_{Ac}$	3.101	(2.949 ; 4.400)	2.247	(1.234 ; 2.511)
$K_{Ac \rightarrow Ac}$	335.20	(90.34 ; 607.23)		
$\alpha_S$	1.203	(0.700 ; 1.638)	1.176	(0.750 ; 1.700)
$\beta_S$	0.228	(0.145 ; 0.316)	0.231	(0.142 ; 0.315)

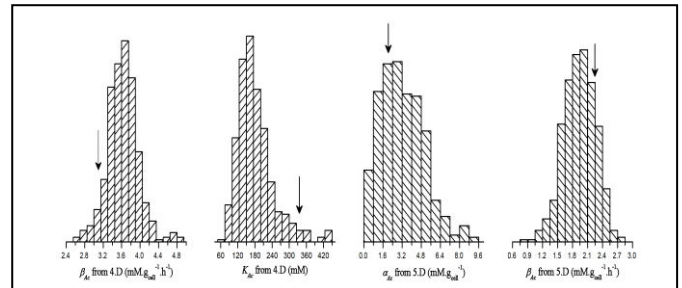


Figure 2. Histograms for the acid parameters.

In the histograms, the arrows indicate where the values of the parameters in Table 7 would be in the distributions. The distributions estimated for the model 4.D (Figure 2.a and 2.b) are not centered on the values obtained by regression. This is most evident with  $K_{Ac}$  (Figure 2.b), where the value of 335.20 mM obtained by regression is located on the tail of the distribution, which by its turn centered around 160 mM. In the case of model 5.D (Figures 2.c and 2.d), the regression values are not exactly centered in the distribution; nevertheless, they are much closer to the center than to the tails. From these results, it is possible to conclude that model 5.D is more robust than model 4.D and most probably describes the reality.

Figure 3 resumes the experimental data as shown in the Figure 1 and the simulation profiles using the model 5.D. Through this model, the polysaccharide formation is not associated to cell growth; however, it is affected by acid production. Figure 1 illustrates that the acid production increases from the batch to the first pulse and to the second pulse; and the profile of cell growth and polysaccharide production tends to decrease. Considering the simulation using the 5.D model, it is possible to verify that corroborates the adjustment of this model (Figure 3). An approach for genome analysis based on sequencing, Fleischmann et al [16], 2000 reported that *H. influenzae* Rd is known to consume carbohydrate such as glucose, fructose and

genes responsible for encoding the complete glycolytic pathway and production of metabolic acids were identified. However, the tricarboxylic acid (TCA) cycle appear to be incomplete and seems to affect cell and polysaccharide production.

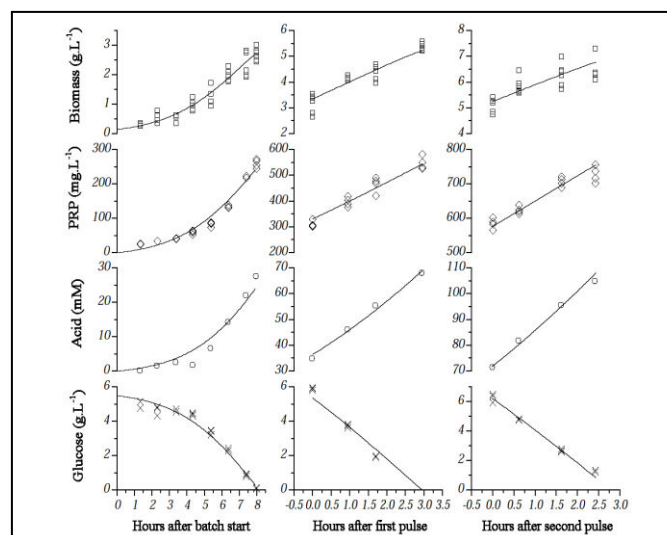


Figure 3: Comparison of the experimental data and the fitted model. The symbols represent the experimental data; the continuous line represent the profile simulates according to the model 5. D. and the columns represent the first batch, after first pulse and after second pulse experiments as shown in the Figure 1.

Takagi et al, 2006 tested some cultivation conditions and found that pH is of fundamental importance in the production of polysaccharide. There is a difference of almost 50% more when the cultivation is carried out with pH control. This fact is in agreement with the results obtained in this study using the 5.D model and may contribute to future experiments as a tool to evaluate the allowed acid rate so that it does not affect cell and polysaccharide production.

## CONCLUSION

By comparing the six different models of acid formation, it was able to determine what is the best assumption for the metabolism of *H. influenzae* type b. Two models were the most likely to be truthful: non-growth-associated formation with acid inhibition and mixed-formation. These two alternatives were used to determine the rules of formation of PRP. Another six alternatives were tested, giving great evidence that PRP is synthesized as a secondary metabolite (independent of cell growth), and that the concentration of acid in the medium

affects its productivity due to metabolic inhibition. The final choice could be made by the evaluation of dispersion of the model parameters. The hypothesis that acid suffers metabolic inhibition showed not to be robust, because the parameter values seemed to be on the edges of the estimated distribution. In this work a model that considers metabolic inhibition by acid on cell growth and PRP synthesis was suggested. It was found that the acid formation follows mixed associated and non-associated pattern and the polysaccharide; the polysaccharide formation is non-associated to cell growth, but inhibited by acid (model 5.D.). The studied models will contribute strongly in understanding the metabolism of this microorganism and to assist in the establishment of the polysaccharide production process.

## NOMENCLATURE

Symbol	Description	Unit
$Ac$	Acid concentration	mM
$\alpha_Q$	Growth-associated constant of compound Q formation	$[Q].g_{cell}^{-1}$
$\beta_Q$	Non-growth-associated constant of compound Q formation	$[Q].g_{cell}^{-1}.h^{-1}$
$K_{Ac \rightarrow Q}$	Inhibition constant of acid on synthesis of compound Q	mM
$K_S$	Substrate saturation constant	$g.L^{-1}$
$\mu$	Specific growth rate	$h^{-1}$
$\mu_{max}$	Maximum specific growth rate	$h^{-1}$
$Ps$	Polysaccharide concentration	$mg.L^{-1}$
$Q$	Generic product concentration	
$S$	Substrate concentration	$g.L^{-1}$
$X$	Biomass concentration	$g.L^{-1}$

## ACKNOWLEDGEMENT

This work was supported by Butantan Foundation and by the technical assistance from Mr. Lourivaldo Ignácio de Souza and Ms. Ana Maria Rodrigues Soares.

## REFERENCES

- Shapiro ED, Ward JI. (1991). The epidemiology and prevention of disease caused by *Haemophilus influenzae* type b. *Epidem.* 13: 113-142.
- Smith AL. (1993). *Haemophilus Influenzae: An important cause of meningitis.* 2. ed. *Mechanisms of microbial Disease.* 15: 235-243.
- Peltola H, Kayhty M, Sivonen A, Makela PH. (1977). *Haemophilus influenzae* type b capsular polysaccharide vaccine in children: a double-blind field study of 100.000

- vaccines 3 Month to 5 years of age in Finland. *Pediatrics*. 60: 730-737.
4. Crisel RM, Baker RS, Dorrman DE. (1975). Capsular polymer of *Haemophilus influenzae* type b. I –structural characterization of the polymer of strain Eagan. *J. Biochem. Chem.* 250: 4926-4930.
  5. Hamidi A, Beurret MF. (2009). Process for producing a capsular polysaccharide for use in conjugate vaccines.
  6. Liu L, Du G, Chen J, Wang M, Sun J. (2008). Enhanced hyaluronic acid production by a two-stage culture strategy based on the modeling of batch and fed-batch cultivation of *Streptococcus zooepidemicus*. *Bioresource Technol.* 99: 8532-8536.
  7. Aiba S, Shoda M. (1969). Reassessment of product inhibition in alcohol fermentation. *J. Ferment. Technol.* 47: 790-794.
  8. Takagi M, Cabrera-crespo J, Zangirolami TC, Raw I, Tanizaki M. (2006). Improved cultivated conditions for polysaccharide production by *H. influenzae* type b. *J. Chem. Technol. Biot.* 81: 182-188.
  9. Cooper GR, Mc Daniel VK. (1966). Evaluation of Glucose Methods. *Enzymol. Biol. et Clin.* 6: 217.
  10. Cintra FO, Takagi M. (2012). Comparison among different sample treatment methods for analysis of molecular weight and concentration of exopolysaccharide produced by *Haemophilus influenzae* type b. *Microbes in Applied Research: Current Advances and Challenges.* 513-517.
  11. Merritt J, Allard G, Toole LO, Swartz R, Licari P. (2000). Development and scale-up of a fedbatch process for the production of capsular polysaccharide from *Haemophilus influenzae*. *J. Biotech.* 81: 189-197.
  12. Ashwell G. (1957). Colorimetric analysis of sugar. *Method in Enzymol.* 3: 73-105.
  13. Luedeking R, Piret EL. (1959). A kinetic study of the lactic acid fermentation: batch process at controlled pH. *J. Biochem. Microbiol.* 1: 393-412.
  14. Pirt SJ. (1965). The maintenance requirement of bacteria in growing cultures. *Proc. Roy. Soc. London.* 163: 224-231.
  15. Motulsky HJ, Christopoulos A. (2003). Fitting models to biological data using linear and nonlinear regression. A practical guide to curve fitting. GraphPad Software Inc, San Diego.
  16. Fleischmann RD, Adams MD, White O, Clayton RA, Kirkness EF, et al. (1995). Whole-genome random sequencing and assembly of *Haemophilus influenzae* Rd. 269: 496-512.